Promega

Innovative bioluminescence assay technology, customized to your requirements.

Fit-for-purpose reagents make it easy.

Let's TALK CUSTOM

HIGH THROUGHPUT

APPLICATION-SPECIFIC DESIGNS

40+ years CUSTOM EXPERIENCE

Selecting a supplier for your drug discovery and development assays can be a challenge—especially a supplier who can adapt to your specific needs. Don't settle for just a supplier. Instead, partner with Promega and work with a custom manufacturer willing to provide you with the scientific expertise, ongoing technical support and quality standards that support your success.

Watch the video or download a PDF:
promega.com/CustomBioluminescence

© 2020 Promega Corporation. All Rights Reserved. 55995314

Bidirectional Reaction Steps in Metabolic Networks: I. Modeling and Simulation of Carbon Isotope Labeling Experiments

Wolfgang Wiechert,* Albert A. de Graaf

Institut für Biotechnologie, Forschungszentrum Jülich, 52425 Jülich GmbH, Germany

Received 7 June 1996; accepted 15 November 1996

Abstract: The extension of metabolite balancing with carbon labeling experiments, as described by Marx et al. (Biotechnol. Bioeng. **49:** 11–29), results in a much more detailed stationary metabolic flux analysis. As opposed to basic metabolite flux balancing alone, this method enables both flux directions of bidirectional reaction steps to be quantitated. However, the mathematical treatment of carbon labeling systems is much more complicated, because it requires the solution of numerous balance equations that are bilinear with respect to fluxes and fractional labeling. In this study, a universal modeling framework is presented for describing the metabolite and carbon atom flux in a metabolic network. Bidirectional reaction steps are extensively treated and their impact on the system's labeling state is investigated. Various kinds of modeling assumptions, as usually made for metabolic fluxes, are expressed by linear constraint equations. A numerical algorithm for the solution of the resulting linear constrained set of nonlinear equations is developed. The numerical stability problems caused by large bidirectional fluxes are solved by a specially developed transformation method. Finally, the simulation of carbon labeling experiments is facilitated by a flexible software tool for network synthesis. An illustrative simulation study on flux identifiability from available flux and labeling measurements in the cyclic pentose phosphate pathway of a recombinant strain of *Zymomonas mobilis* concludes this contribution. © 1997 John Wiley & Sons, Inc. *Biotechnol Bioeng* **55:** 101–117, 1997.
Keywords: stationary flux analysis; metabolite flux balancing; ^{13}C isotope labeling experiments; NMR; metabolic engineering

INTRODUCTION

Stationary Flux Analysis

The quantitation of metabolic fluxes in the central metabolism of cells has always been of great interest in physiological research. In the last few years, increasing activities in the field of metabolic engineering (Bailey, 1991; Stephanopoulos et al., 1991, 1993) emphasize the need for precise and extensive quantitation methods in biotechnology. However, only recently have experimental methods become available, enabling a sufficient amount of high precision measurement data to be gathered for this task (Rizzi et al., 1996; Weuster-Botz and de Graaf, 1996; Wiechert and de Graaf, 1996).

This contribution concentrates on the carbon isotope labeling approach for flux quantitation under metabolic steady-state conditions (Marx, 1996; Wiechert and de Graaf, 1996). In this situation, neither mechanistic assumptions about enzyme and transport kinetics, nor the knowledge of energy yields are required for flux determination.

Consequently, stationary flux estimates computed from labeling experiments are expected to exhibit a high degree of reliability. The practical aspects of stationary flux analysis and its relation to dynamic modeling are discussed in Wiechert and de Graaf (1996).

Metabolite Flux Balancing

The quantitation of intracellular fluxes in vivo requires measurement techniques to be available that do not influence the metabolic state of the observed microorganism. When defined and stable physiological conditions have been established inside a bioreactor, all relevant fluxes between the cell interior and the surrounding medium—like substrate uptake, product formation, biomass growth, or gas efflux—can be measured with standard analytical instruments (Schugerl, 1991). These fluxes are henceforth called the *extracellular* fluxes as opposed to the *intracellular* fluxes that are to be quantitated.

A well-established approach to intracellular flux determination based on these measured extracellular flux data is given by metabolite flux balancing (Goel et al., 1993; Jorgensen, 1995; Vallino and Stephanopoulos, 1992; Varma et al., 1994). However, it turned out that the available extracellular flux measurement data is not always sufficient to determine all intracellular fluxes in the central metabolism without further simplifying assumptions on enzyme activities and energy yields (Goel et al., 1993; Jorgensen, 1995; Roels, 1983; Vallino, 1991).

* *Present address:* IMR, Abteilung Simulationstechnik, Universität-GH Siegen, 57068 Siegen, Germany; telephone: 0271/740-4727; fax: 0271/740-2365; e-mail: wiechert@simtec.imr.mb.uni-siegen.de.
Correspondence to: W. Wiechert
Contract grant sponsor: Stiftung Volkswagenwerk

© 1997 John Wiley & Sons, Inc. CCC 0006-3592/97/010101-17

Clearly, such assumptions restrict the reliability of stationary flux determination. On the other hand, such assumptions can only be left out if they are compensated by additional measurements.

Carbon Isotope Labeling Technique

Another source of information that has long been used in physiological research is given by the selective enrichment of intracellular metabolites by carbon isotopes like ^{13}C or ^{14}C (also called the *label*). By the *fractional enrichment* of label in the *i*th carbon atom position of some metabolite M we henceforth mean the percentage of M-molecules with a ^{13}C isotope at position *i*.

To obtain this information, a so-called *labeling experiment* (also denoted as *tracer experiment*) is performed (Anderson, 1983; Blum and Stein, 1982; Lambrecht and Rescigno, 1983; Wiechert and de Graaf, 1996). In such an experiment a substrate with known labeling state (e.g., 1-^{13}C glucose) is fed into the system during a metabolic stationary state. The label then becomes distributed all over the metabolic network until the fractional labeling in all intracellular metabolite pools equilibrates (*isotopic steady state*). In this situation the fractional enrichments at the carbon atom positions of certain intracellular metabolites are determined.

An important improvement of the carbon labeling method has recently been achieved by the isolation and hydrolization of intracellular polymers like protein or nucleic acids (Eisenreich et al., 1993; Ekiel et al., 1983; Marx et al., 1996; Szyperski, 1995). The subsequent ^{13}C NMR analysis of amino acids and ribonucleotides makes the collection of a formerly unattainable amount of high-precision fractional labeling data possible (Marx et al., 1996). Clearly, the measured data corresponds directly to the labeling state of the corresponding precursor metabolites in central metabolism. Details on the experimental and analytical procedures and the validity of this approach can be taken from other works (Marx et al., 1996; Wiechert, 1996a; Wiechert and de Graaf, 1996).

An important feature of this new labeling technique is that the experiment takes place in a bioreactor (Marx et al., 1996) so that the extracellular fluxes can be measured in a complementary manner. Consequently, the metabolite flux balancing technique for flux determination can now be combined, to a large extent, with the carbon isotope labeling technique.

Modeling and Evaluation of Carbon Isotope Labeling Experiments

The metabolite flux balancing technique—that is, the exploitation of linear relations in flux networks—is well understood from a computational and statistical point of view (Chatterjee and Hadi, 1988; van Heijden et al., 1994a, 1994b; Vallino, 1991). In contrast, isotope labeling experiments lead to substantially more complex nonlinear models (Anderson, 1983; Blum and Stein, 1982; Wiechert and de Graaf, 1996). Only rudimentary methods for the computational and statistical treatment of such models have been developed in the past and all are all restricted to specific metabolic systems (Blum and Stein, 1982; Crawford and Blum, 1983; Portais et al., 1995; Sharfstein et al., 1994; Zupke and Stephanopoulos, 1995). Only recently have some universal modeling efforts been undertaken to describe metabolic isotope labeling systems in a more general way (Schuster et al., 1992; Wiechert and de Graaf, 1993; Zupke and Stephanopoulos, 1994). Moreover, some computer-supported tools have been developed to handle the additional complexity and to simulate experiments (Schuster et al., 1992; Weichert, 1994; Zupke and Stephanopoulos, 1994).

However, these approaches make little effort to establish general algorithms for systems analysis and statistical evaluation of experiments. In particular the numerical stability of the implemented algorithms has not yet been sufficiently analyzed. Moreover, universally applicable statistical results on sensitivity analysis, computation of confidence regions, and parameter identifiability analysis, especially for bidirectional reaction steps, have not yet been obtained. This is a very unsatisfactory situation because most of the labeling data available with the experimental techniques just described require the development of flexible computational and statistical methods that take advantage of redundant measurement data.

Bidirectional Reaction Steps

In principle, any reversible reaction having a small free energy difference, $\Delta G'$, in vivo (that may well differ from the standard free Gibbs energy, $\Delta G^{0\prime}$) (Mavrovouniotis, 1991; Westerhoff and van Dam, 1987) has the potential to proceed in both directions at the same time. If the forward and backward reactions take place simultaneously we speak of a *bidirectional* reaction step (Wiechert and de Graaf, 1996). On the other hand, an irreversible reaction with large ΔG in vivo can safely be assumed to be *unidirectional.* However, only a few reaction steps in the central metabolism allow this assumption. Consequently, the majority should be examined for their bidirectionality.

A distinguishing feature of the carbon labeling technique compared to metabolite flux balancing is that both directions of a reaction step influence the labeling state of the system (Wiechert et al., 1995). This has already been recognized in the past, so many published models contain some bidirectional steps (Chatham et al., 1995; Crawford and Blum, 1983; Rabkin and Blum, 1985; Stein and Blum, 1979; Zupke and Stephanopoulos, 1994); however, this matter has never been investigated extensively. In particular, it turns out that the presence of highly reversing bidirectional steps leads to severe prob-

lems for the numerical treatment of models and nonlinear statistical data evaluation (Marx et al., 1996; Schuster et al., 1993; Wiechert and de Graaf, 1996).

Aims of This Study

We have developed and present here a universal modeling, simulation, and data analysis framework for metabolic flux analysis by stationary carbon isotope labeling experiments using fractional enrichment data. Although the model structure has already been introduced in rudimentary form in Marx et al. (1996), the technical, computational, and statistical details as well as an extensive investigation of bidirectional reaction steps could not be presented in that study. The purpose of this article now is to examine extensively the following items:

1. A universal modeling approach for stationary carbon isotope labeling experiments will be presented that allows the use of fractional enrichment data in addition to conventional measurements of extracellular fluxes. For the first time, the effect of bidirectional reaction steps will be considered to its full extent. A simple and precise formal language will then be defined to express all structural and physiological assumptions made about the system.
2. The complex model equations arising will be represented in a concise matrix notation that is well suited for further mathematical systems analysis (cf. Wiechert, 1996a, 1996b). Using the formal language introduced a completely automated computer generation of all required matrices has been achieved.
3. The influence of bidirectional reaction steps on the system's labeling state will be investigated in detail. It will be demonstrated that, for practical applications, numerical stability problems have to be expected, which are caused by reaction steps with large bidirectional fluxes.
4. The problems of accessible labeling states, identifiability of fluxes, and redundancy of measurement data will be discussed and demonstrated with an illustrative simulation example.

Due to the complexity and broadness of scope covered the results will be presented in this and a sequel article (Wiechert et al., 1997). Part I introduces the general modeling and simulation framework using some rather simple examples to demonstrate the most important systemic features of metabolic labeling systems and bidirectional fluxes. The sequel (Part II) will then present the details of flux estimation from measured data and statistical analysis. In particular, the stability problems will be completely solved by a sophisticated numerical algorithm, which will then be applied to a complex flux estimation example for *Corynebacterium glutamicum* to demonstrate its power and limitations. The reader who is interested in further results on model simplification, redundancy, and identifiability analysis is referred to other published works (Wiechert, 1995, 1996a, 1996b).

ASSUMPTIONS ABOUT THE BIOLOGICAL SYSTEM

The assumptions about the biological system required for modeling isotope labeling are rather weak compared with those required for dynamic modeling; that is, no assumptions about enzyme or transport kinetics or energy yield coefficients have to be made. However, the few assumptions should be stated clearly:

(A1) As for material balancing models the basic assumption of compartmental modeling (Anderson, 1983; Holzhutter, 1985) must hold; that is, the system state can be represented by the concentrations of a finite set of homogeneously distributed pools. In our case, there is one pool for each carbon atom position of each intracellular metabolite considered. For instance, the total of all ^{12}C and ^{13}C isotopes at the second carbon position of the intracellular fructose-6-phosphate molecules comprise one pool. In case of intracellular compartmentation, pools may have to be further subdivided (see, e.g., Blum and Stein, 1982).

(A2) The observed microbial system must be kept in a well-defined stationary physiological state during the measurement procedure. This can take a considerably long time depending on the measurement technique used (Wiechert, 1996a). However, the maintenance of controlled chemostatic or nutristatic cultures over long periods is a routine procedure.

(A3) For the metabolic pathways of interest, all relevant biochemical transformations must be known with respect to the reaction steps involved and the fate of all carbon atoms within each step. For the central metabolism this knowledge is well established and can be taken from any biochemistry textbook (Stryer, 1988).

(A4) There are no measurable isotopic mass effects. This means that the labeling state of a molecule does not influence the rate of its enzymatic conversion. According to current knowledge this is true at least of liquid phase reaction systems. However, it should be mentioned here that mass effects have been observed in certain situations for small molecules, like CO_2 (O'Leary, 1982; Winkler et al., 1982).

The structure of the general metabolic model presented in what follows relies solely on **(A3). (A1)** and **(A2)** then guarantee the validity of balance equations, and **(A4)** states that no mass correction factors have to be introduced into the balance equations. However, the degree of freedom of the flux state space can be reduced substantially by making further assumptions about reaction steps:

- A large standard free energy term, $\Delta G^{0\prime}$, may justify the assumption of irreversibility in vivo; that is, the corresponding reaction step may be considered unidirectional.
- Rapid equilibrium conditions may be assumed for certain highly reversible enzymatic steps; for example, isomerase and epimerase in the pentose phosphate pathway (Wood, 1985).
- Stoichiometric coefficients for energy yields may be assumed to be known as is usually done in metabolite flux balancing (Vallino, 1991).
- Reduction equivalents like NADH and NADPH may be balanced in detail; that is, all producing and consuming reactions are assumed to be known (Vallino and Stephanopoulos, 1992).

Such assumptions are optional in the framework to be described and should be carefully documented to achieve transparency of the modeling process and reproducibility of results. If in doubt, an assumption should be left out, thereby increasing the number of unknown fluxes to be estimated. On the other hand, if all fluxes turn out to be identifiable from the measured data, flux properties can be verified experimentally. The modeling framework for expressing structural and quantitative assumptions on the metabolic network is introduced in the following sections.

AN ILLUSTRATIVE EXAMPLE

Before introducing the general metabolite and carbon flux equations in their matrix notation a simple example will be discussed. It serves to demonstrate the principles of intracellular flux estimation from fractional carbon labels combined with measured extracellular fluxes. Because of the example's low dimensionality the obtained properties can be easily represented graphically. Moreover, the potential for estimating both directions of bidirectional fluxes is illustrated and the general numerical and statistical problems to be solved later on are introduced.

The reaction network and its carbon atom transitions can be taken from Figure 1. The network consists of an input metabolite A with a known labeling state, intracellular intermediates B and C and an output metabolite D, each with two carbon atoms. The network represents a rudimentary metabolic cycle with different fates of carbon atoms in its branches given by V_2 and V_3. V_1 is the system input flux (and thus measurable), V_2 and V_3 are intracellular, and V_4 is an output flux.

An input flux like V_1 is always assumed to be unidirectional because external sources are always considered inexhaustible in material balancing. Similarly, output fluxes like V_4 are not allowed to reverse their direction. The intracellular flux V_3 is assumed to be unidirectional, whereas V_2 takes place in both directions. This situation is not unusual in complex reaction networks where V_2 and V_3 may represent reaction sequences with only one branch containing highly reversible steps. For example, V_3 may stand for a part of glycolysis, whereas V_2 represents the pentose phosphate pathway.

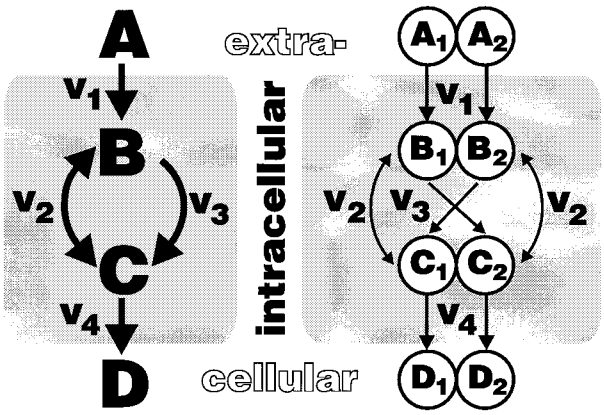

Figure 1. A simple example network. Left: metabolite view. Right: carbon atom view. The extracellular flux, v_1, and the labels, b_1, c_1, are assumed to be measurable. The input labels, a_1, a_2, are known.

State Variables and Assumptions About Fluxes

The fluxes within the system will be described in terms of flux variables, $v_i \geq 0$. More precisely, a distinction is made between both directions of each flux by using the symbols $v_i^{\rightarrow}$ and $v_i^{\leftarrow}$, respectively. These values are henceforth called the forward and backward fluxes. The assumptions about the example network are now given by:

$$\begin{aligned} v_1^{\leftarrow} &= 0 \quad \text{because } V_1 \text{ is an input flux} \\ v_3^{\leftarrow} &= 0 \quad \text{because } V_3 \text{ is assumed to be unidirectional} \\ v_4^{\leftarrow} &= 0 \quad \text{because } V_4 \text{ is an output flux} \end{aligned} \tag{1}$$

The fractional labeling at each carbon atom position of the intracellular metabolites is denoted by b_1, b_2, c_1, $c_2 \in [0, 1]$. The known system input is specified by a_1, a_2. For example, a substrate A, which is 100% labeled at the first carbon atom position, is described by $a_1 = 1.0$, $a_2 = 0.0$. The output metabolite D is not required for formulating the balance equations because its labeling state will always equal that of its precursor C.

Flux and Label Balances

Metabolite and label balances can now be stated according to assumptions **(A1)** and **(A2).** The metabolite fluxes from and to each intracellular metabolite pool must add up to zero in the stationary state (Hofmeyr, 1986). Using Eqs. (1) this gives rise to the following linear metabolite balance equations for the metabolite pools B and C:

$$\begin{aligned} \text{B:} \quad & v_1^{\rightarrow} + v_2^{\leftarrow} = v_2^{\rightarrow} + v_3^{\rightarrow} \\ \text{C:} \quad & v_2^{\rightarrow} + v_3^{\rightarrow} = v_2^{\leftarrow} + v_4^{\rightarrow} \end{aligned} \tag{2}$$

from which it follows:

$$\begin{aligned} v_3^{\rightarrow} &= v_1^{\rightarrow} - v_2^{\rightarrow} + v_2^{\leftarrow} \\ v_4^{\rightarrow} &= v_1^{\rightarrow} \end{aligned} \tag{3}$$

This leaves 3 degrees of freedom that may be represented by the (linearly) independent variables $v_1^{\rightarrow}$, $v_2^{\rightarrow}$, and $v_2^{\leftarrow}$, henceforth called the *free fluxes.*

To establish the carbon label balances, the (forward) atom transition V_2: $\mathsf{B}_1 \rightarrow \mathsf{C}_1$, affecting the first carbon atoms of B and C, is considered. It carries the amount of $v_2^{\rightarrow} \cdot b_1$ labeled atoms and $v_2^{\rightarrow} \cdot (1 - b_1)$ unlabeled atoms per time unit. Herein assumption **(A4)** is used; that is, no isotope mass effects occur. The term $v_2^{\rightarrow} \cdot b_1$ contributes to the label balances of B_1 and C_1, but with opposite signs. The complete set of all equations for the four intracellular carbon atom pools then is:

$$\begin{aligned} \mathsf{B}_1\text{:}\quad 0 &= v_1^{\rightarrow} a_1 - v_2^{\rightarrow} b_1 + v_2^{\leftarrow} c_1 - v_3^{\rightarrow} b_1 \\ \mathsf{B}_2\text{:}\quad 0 &= v_1^{\rightarrow} a_2 - v_2^{\rightarrow} b_2 + v_2^{\leftarrow} c_2 - v_3^{\rightarrow} b_2 \\ \mathsf{C}_1\text{:}\quad 0 &= \qquad v_2^{\rightarrow} b_1 - v_2^{\leftarrow} c_1 + v_3^{\rightarrow} b_2 - v_4^{\rightarrow} c_1 \\ \mathsf{C}_2\text{:}\quad 0 &= \qquad v_2^{\rightarrow} b_2 - v_2^{\leftarrow} c_2 + v_3^{\rightarrow} b_1 - v_4^{\rightarrow} c_2 \end{aligned} \tag{4}$$

It should be noticed that this consideration is true only when molar units are used for the flux variables because these are interpreted both as metabolite fluxes in Eq. (2) and as carbon atom fluxes in Eq. (4).

Computation of Fractional Labeling and Flux Determination

The balance equations can now be used to represent all fractional labels in terms of fluxes. To keep the number of algebraic terms in the example small, we restrict ourselves to the special case:

$$a_1 = 1,\ a_2 = 0 \tag{5}$$

From Eqs. (4) and (5) one derives:

$$1 = a_1 + a_2 = b_1 + b_2 = c_1 + c_2 \tag{6}$$

Using Eqs. (6) and (3), the labels are expressed as a function of the free fluxes:

$$\begin{aligned} b_1 &= [(v_1^{\rightarrow})^2 + 2v_1^{\rightarrow}v_2^{\leftarrow} - v_2^{\rightarrow}v_2^{\leftarrow} + (v_2^{\leftarrow})^2]/\delta, & b_2 &= 1 - b_1 \\ c_1 &= [(v_1^{\rightarrow}v_2^{\rightarrow} + v_1^{\rightarrow}v_2^{\leftarrow} - v_2^{\rightarrow}v_2^{\leftarrow} + (v_2^{\leftarrow})^2]/\delta, & c_2 &= 1 - c_1 \end{aligned} \tag{7}$$

with $\delta = (v_1^{\rightarrow})^2 + 3v_1^{\rightarrow}v_2^{\leftarrow} - 2v_2^{\rightarrow}v_2^{\leftarrow} + 2(v_2^{\leftarrow})^2$

Eq. (7) determines the relative flux distribution over the metabolic network. However, only a single flux measurement is sufficient to determine the absolute values of all fluxes. To this end, we will assume in the following that the substrate uptake, $v_1^{\rightarrow}$, is known from measurements and all fluxes are scaled to $v_1^{\rightarrow} = 1$.

This leaves $v_2^{\rightarrow}, v_2^{\leftarrow}$ to be determined from measurements. By Eq. (6), b_2, c_2 are redundant with b_1, c_1 so that at least one label fraction from B and C—say b_1 and c_1—must be measured to achieve this goal. Then, the correspondence:

$$\gamma : (v_2^{\rightarrow}, v_2^{\leftarrow}) \rightarrow (b_1, c_1) \tag{8}$$

defined by Eq. (7), completely characterizes the system. To determine all fluxes from b_1, c_1, the mapping γ must be proven to be one-to-one. It can easily be derived from Eqs. (4) and (6) that γ^{-1} is given by:

$$\begin{aligned} v_2^{\leftarrow} &= -(1 - b_1)/(c_1 - b_1) \cdot v_1^{\rightarrow} \\ v_2^{\rightarrow} &= (1 - b_1 - c_1)/(1 - 2b_1) \cdot (v_1^{\rightarrow} + v_2^{\leftarrow}) \end{aligned}$$

This explicit solution for the flux determination problem already shows how both forward and backward fluxes of bidirectional reactions can be computed from ^{13}C labeling data. With conventional measurement techniques only the corresponding net fluxes would be observable!

Accessible Labeling States

Figure 2a shows the one-to-one correspondence, γ, using a two-dimensional superposition of contour plots (cf. Zupke and Stephanopoulos, 1994). As can be seen immediately, not all labeling states (b_1, c_1) of the system are accessible by fluxes $v_2^{\rightarrow}, v_2^{\leftarrow} \geq 0$. It can be derived from Eq. (7) that the set of *accessible labeling states* is given by:

$$b_1 \leq 1,\ b_1 > c_1,\ b_1 \geq 1 - c_1 \tag{9}$$

Moreover (as can be seen from Fig. 2a), the boundary line $b_1 = c_1$ is only asymptotically reached when $v_2^{\rightarrow}$ and $v_2^{\leftarrow}$ simultaneously tend to infinity. This observation has far-reaching consequences for practical flux determination:

1. If pools B and C are at nearly isotopic equilibrium, the determined fluxes $v_2^{\rightarrow}$ and $v_2^{\leftarrow}$ become extremely sensitive with respect to measurement errors. A small measurement deviation then leads to an ill-determined flux estimation, which in extreme cases may vary within some orders of magnitude.
2. The measured labels may even be situated in the inaccessible region (shaded gray in Fig. 2a) due to measurement errors. In this situation, the most suitable flux estimation is obtained from the projection of the point corresponding to the measured values to the nearest boundary line of the accessible region. If this happens to be the line $b_1 = c_1$ this flux estimation is given by $v_2^{\rightarrow} = v_2^{\leftarrow} = \infty$!

These problems are quite frequently encountered in carbon labeling networks because the accessible region can become quite narrow in practice (compare to Wiechert, (1996a) for another example). The aforementioned consideration shows that dramatic numerical and statistical problems will arise in the numerical quantita-

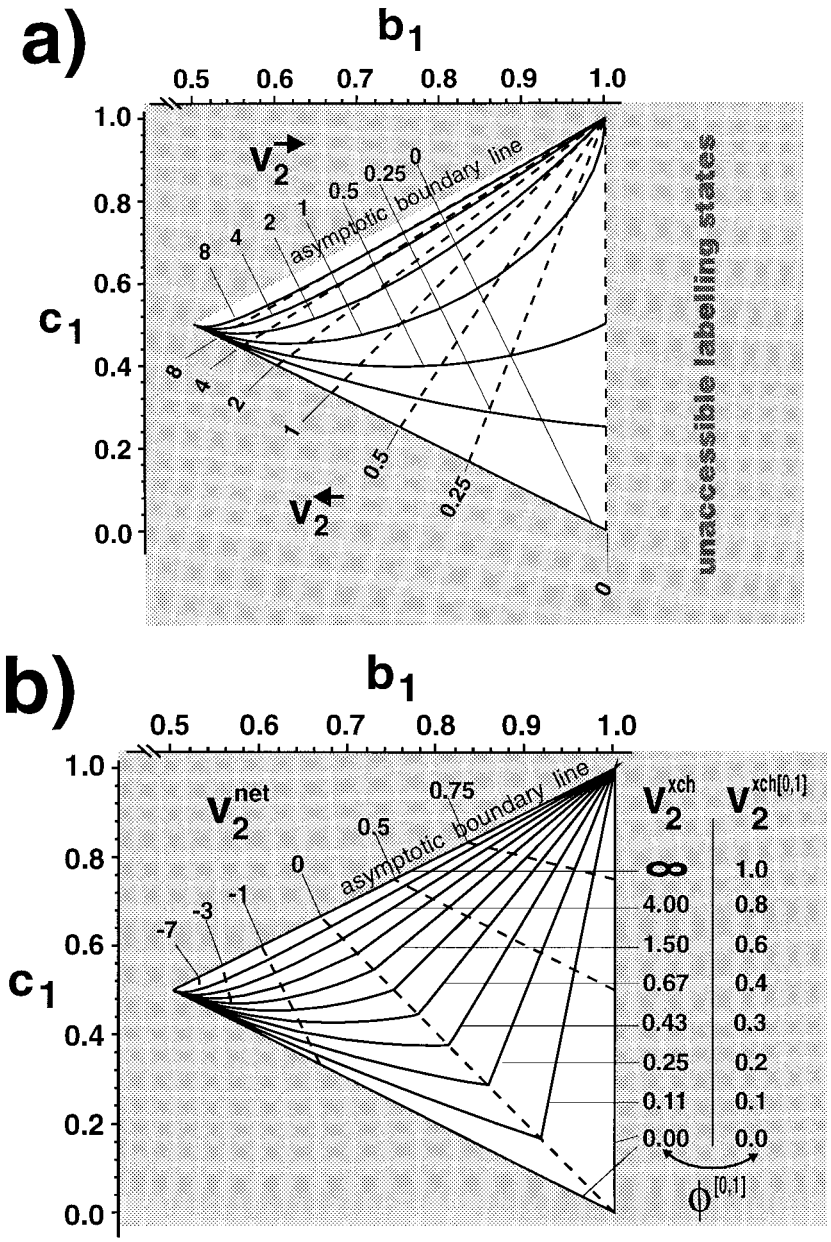

Figure 2. Representation of the one-to-one correspondences between three different flux coordinate systems and the labeling state in the example of Figure 1. (a) γ: $(v_2^{\rightarrow}, v_2^{\leftarrow}) \rightarrow (b_1, c_1)$; (b) $\phi \circ \gamma$: $(v_2^{\rightarrow}, v_2^{\leftarrow}) \rightarrow (b_1, c_1)$; and $\phi^{[0,1]_1} \circ \phi \circ \gamma$: $(v_2^{\rightarrow}, v_2^{\leftarrow}) \rightarrow (b_1, c_1)$. In each case, all fluxes are normalized to $v_1^{net} = 1$.

tion of bidirectional fluxes. The following concepts were developed to solve these problems in a convenient way.

A Suitable Definition of Exchange Fluxes

Forward and backward fluxes are unsuitable variables for the description of a bidirectional reaction step not only for numerical reasons, but also for the practical interpretation of flux values. To obtain a more suitable representation of the bidirectional step V_2 we take the familiar *net flux*, v_2^{net}, and a newly defined *exchange flux*, v_2^{xch}, given by:

$$\begin{aligned} v_2^{net} &= v_2^{\rightarrow} - v_2^{\leftarrow} \\ v_2^{xch} &= \min(v_2^{\rightarrow}, v_2^{\leftarrow}) \end{aligned} \tag{10}$$

Figure 3 illustrates how v_2^{xch} quantitates the amount of flux common to both directions $v_2^{\rightarrow}$ and $v_2^{\leftarrow}$. Several advantages of this definition, as compared with other possible definitions (e.g., from Schuster et al., 1992), are discussed in Wiechert (1996a). In particular, one can easily prove the transformation rule:

$$\begin{aligned} v_2^{\rightarrow} &= v_2^{xch} - \min(-v_2^{net}, 0) \\ v_2^{\leftarrow} &= v_2^{xch} - \min(v_2^{net}, 0) \end{aligned}$$

showing that the mapping:

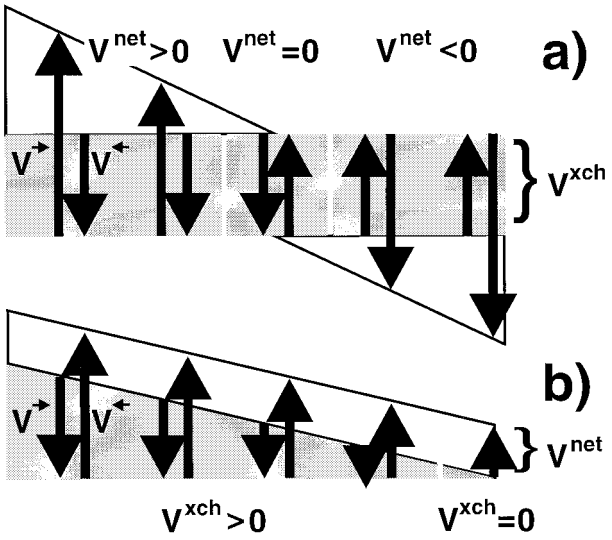

Figure 3. Definition of exchange fluxes for bidirectional reaction steps showing forward and backward flux for (a) fixed exchange flux and varying net flux and (b) fixed net flux and varying exchange flux.

$$\phi : (v_2^{net}, v_2^{xch}) \rightarrow (v_2^{\rightarrow}, v_2^{\leftarrow}) \tag{11}$$

is really a coordinate transformation between the *natural flux coordinates* $(v_2^{\rightarrow}, v_2^{\leftarrow})$ and the *application flux coordinates* (v_2^{net}, v_2^{xch}).

The Role of Exchange Fluxes

The one-to-one mapping:

$$\gamma \circ \phi : (v_2^{net}, v_2^{xch}) \rightarrow (b_1, c_1)$$

resulting from Eqs. (8) and (11) is represented in Figure 2b. It turns out that the asymptotically accessible boundary line $b_1 = c_1$ is now exactly characterized by $v_2^{xch} = \infty$, whereas the net flux v_2^{net} varies along this line. This effect is expected because a large exchange flux, v_2^{xch}, means a rapid equilibrium between the pools B_1 and C_1 connected by V_2; that is, their labeling state will be asymptotically equal.

For flux determination the new definitions of Eq. (10) have the consequence that, in the situation where (b_1, c_1) is situated near the boundary line $b_1 = c_1$, a measurement error will lead to a comparably well-determined net flux, whereas the exchange flux can only be estimated within a large confidence interval. This is a valuable result for practical purposes because the net flux is always an important quantity. However, if the measurement of (b_1, c_1) lies beyond the boundary $b_1 = c_1$ this will lead to an exchange flux estimated to be infinite. For the computational treatment of the system this is a troublesome situation, because possible infinite values will lead to unpredictable and unstable numerical results.

Another Exchange Flux Definition

This problem can be overcome for numerical implementation purposes by mapping the theoretically possible value range $[0, \infty]$ of v_2^{xch} to the finite range [0, 1] using the hyperbolic transformation:

$$v_2^{xch} \rightarrow v_2^{xch[0,1]} = v_2^{xch}/(\beta + v_2^{xch})$$

with some positive constant β. Such a rescaling to a bounded range of values is well known as a *compactification* operation in mathematical theory (Ahlfors, 1979). The inverse transformation leads to the one-to-one mapping:

$$\begin{aligned}\phi_\beta^{[0,1]} : (v_2^{net}, v_2^{xch[0,1]}) &\rightarrow (v_2^{net}, v_2^{xch}) \\ &= (v_2^{net}, \beta \cdot v_2^{xch[0,1]}/(1 - v_2^{xch[0,1]}))\end{aligned} \tag{12}$$

The new coordinates $(v_2^{net}, v_2^{xch[0,1]})$ will be denoted as the *numerical flux coordinates.* A representation of the resulting map:

$$\gamma \circ \phi \circ \phi_\beta^{[0,1]} : (v_2^{net}, v_2^{xch[0,1]}) \rightarrow (b_1, c_1)$$

obtained from Eqs. (8), (11), and (12) for $\beta = 1$ is given in Figure 2b. Concerning the choice of β, it turned out in numerical studies that good sensitivity results are always achieved when β was chosen in the order of magnitude of the system input flux; that is, v_1^{net} in the example.

The boundary line $b_1 = c_1$ is now given by $v_2^{xch[0,1]} = 1$, and even when measurement errors occur the sensitivity of the numerical exchange flux, $v_2^{xch[0,1]}$, with respect to measurement errors, remains bounded. Moreover, it can be generally shown that, as a function of $v_2^{xch[0,1]}$ and v_2^{net}, the labeling state (b_1, c_1) can be differently continued in $v_2^{xch[0,1]} = 1$ (Wiechert, 1996a). Thus, from a mathematical viewpoint, the asymptotic boundary line $b_1 = c_1$ can now be treated like all other points in the accessible region given by Eqs. (9). This enables numerically stable algorithms for simulation and flux estimation to be implemented even when large exchange fluxes occur (see Appendix B of Part II of Wiechert et al. [1997] for more details).

DEVELOPMENT OF A GENERAL MATHEMATICAL MODEL

The developed universal model for carbon flux in metabolic networks is now explained by generalizing the concepts presented for the simple example. It makes extensive use of matrix calculus to obtain a concise notation. The final model essentially consists of Eq. (15) expressing structural properties of the metabolic carbon atom network (Reder, 1988) and Eqs. (19) and (20) expressing all quantitative assumptions made about net and exchange fluxes.

An important property of the general model is that all vectors and matrices can be automatically generated from the structural input and the assumptions made. Some details of the corresponding computer implementation are given in the Appendix. A summary of all model equations introduced in this section will be presented in Part II (Wiechert et al., 1997).

State Variables

The first state variables introduced for formulating the model are the forward and backward fluxes of each reaction step. They are comprised of the natural flux state vectors $\mathbf{v}^{\rightarrow}$ and $\mathbf{v}^{\leftarrow}$ (of equal dimension). In the simple example from Figure 1 these vectors are $\mathbf{v}^{\rightarrow} = (v_1^{\rightarrow}, v_2^{\rightarrow}, v_3^{\rightarrow}, v_4^{\rightarrow})^T$ and $\mathbf{v}^{\leftarrow} = (v_1^{\leftarrow}, v_2^{\leftarrow}, v_3^{\leftarrow}, v_4^{\leftarrow})^T$. On the other hand, as has been discussed in the preceding section, $\mathbf{v}^{\rightarrow}$, $\mathbf{v}^{\leftarrow}$ are rather inconvenient for a practically useful interpretation of the results achieved. For this reason, the application flux coordinate system is introduced by analogy to Eqs. (10). The minimum now has to be applied componentwise to obtain the transformation:

$$\Phi: \begin{pmatrix} \mathbf{v}^{\text{net}} \\ \mathbf{v}^{\text{xch}} \end{pmatrix} \rightarrow \begin{pmatrix} \mathbf{v}^{\rightarrow} \\ \mathbf{v}^{\leftarrow} \end{pmatrix} = \begin{pmatrix} \mathbf{v}^{\text{xch}} - \min(-\mathbf{v}^{\text{net}}, 0) \\ \mathbf{v}^{\text{xch}} - \min(\mathbf{v}^{\text{net}}, 0) \end{pmatrix} \quad (13)$$

Similarly, the numerical flux coordinate system is obtained with the compactification transformation:

$$\Phi_{\beta}^{[0,1]}: \begin{pmatrix} \mathbf{v}^{\text{net}} \\ \mathbf{v}^{\text{xch}[0,1]} \end{pmatrix} \rightarrow \begin{pmatrix} \mathbf{v}^{\text{net}} \\ \mathbf{v}^{\text{xch}} \end{pmatrix} = \begin{pmatrix} \mathbf{v}^{\text{net}} \\ \beta \cdot \mathbf{v}^{\text{xch}[0,1]} / (\mathbf{1} - \mathbf{v}^{\text{xch}[0,1]}) \end{pmatrix} \quad (14)$$

Here, the division has to be carried out componentwise (where $\mathbf{1}$ denotes the vector with all entries being 1), and β is a constant chosen in the order of magnitude of the substrate uptake flux.

The second state variable is the vector $\mathbf{x}$ of fractional labeling within each (enumerated) carbon atom in the intracellular metabolites. Furthermore, the constant vector $\mathbf{x}^{\text{inp}}$ of input labels comprising the known fractional labels of all carbon atoms that are fed into the system is required. In the example in Figure 1 we have $\mathbf{x} = (b_1, b_1, c_1, c_2)^T$ and $\mathbf{x}^{\text{inp}} = (a_1, a_2)^T$.

Carbon Label Balances

As can be seen from Eq. (4) the carbon isotope balance equations have a bilinear structure with respect to $\mathbf{x}$, $\mathbf{x}^{\text{inp}}$ and $\mathbf{v}^{\rightarrow}$, $\mathbf{v}^{\leftarrow}$; that is, all terms are of type $\pm\mathbf{v}_i \cdot \mathbf{x}_j$. To arrange the signs ± 1 in a tabular structure the *atom transition matrices* $\mathbf{P}_i^{\rightarrow}$, $\mathbf{P}_i^{\leftarrow}$ (for intracellular transitions) and $\mathbf{P}_i^{\text{inp}}$ (for input label transitions) are introduced. The precise definition of $\mathbf{P}_i^{\rightarrow}$ must take into account the fact that an intracellular multimolecular reaction step like A + A → B + C can multiply affect one carbon atom pool:

$$(\mathbf{P}_i^{\rightarrow})_{j,k} = \begin{cases} l & \text{if the } i\text{th forward reaction supplies pool } j \text{ with } l \text{ carbon atoms from pool } k; \\ -l & \text{if } j = k \text{ and the } i\text{th forward reaction takes } l \text{ carbon atoms from pool } j; \\ 0 & \text{elsewhere} \end{cases}$$

$\mathbf{P}_i^{\leftarrow}$ is similarly defined. The same holds for $\mathbf{P}_i^{\text{inp}}$ which collects all indices of carbon atom transitions between an extracellular and an intracellular pool.

In the example of Figure 1 some of the intracellular and input carbon transition matrices are given by (with points denoting zero entries):

$$\mathbf{P}_2^{\rightarrow} = \begin{pmatrix} -1 & . & . & . \\ . & -1 & . & . \\ 1 & . & . & . \\ . & 1 & . & . \end{pmatrix}, \mathbf{P}_2^{\leftarrow} = \begin{pmatrix} . & . & 1 & . \\ . & . & . & 1 \\ . & . & -1 & . \\ . & . & . & -1 \end{pmatrix},$$

$$\mathbf{P}_1^{\text{inp}} = \begin{pmatrix} 1 & . \\ . & 1 \\ . & . \\ . & . \end{pmatrix}$$

The scalar-matrix-vector product, $\mathbf{v}_i^{\rightarrow} \cdot \mathbf{P}_i^{\rightarrow} \cdot \mathbf{x}$, is now exactly the vector of all bilinear terms $\pm\mathbf{x}_j\mathbf{v}_i^{\rightarrow}$ that are contributed by $\mathbf{v}_i^{\rightarrow}$ to all intracellular pools in the system. Similarly, $\mathbf{v}_i^{\rightarrow} \cdot \mathbf{P}_i^{\text{inp}} \cdot \mathbf{x}^{\text{inp}}$ consists of all bilinear terms corresponding to label input. Combining all these terms we end up with the general carbon flux balance equation in matrix notation:

$$\left(\sum_i \mathbf{v}_i^{\rightarrow} \cdot \mathbf{P}_i^{\rightarrow} + \sum_i \mathbf{v}_i^{\leftarrow} \cdot \mathbf{P}_i^{\leftarrow} \right) \cdot \mathbf{x} + \left(\sum_i \mathbf{v}_i^{\rightarrow} \cdot \mathbf{P}_i^{\text{inp}} \right) \cdot \mathbf{x}^{\text{inp}} = \mathbf{0} \quad (15)$$

It should be observed that $\mathbf{P}_i^{\rightarrow} = -\mathbf{P}_i^{\leftarrow}$ does not hold. Consequently, the change of the signs of both $\mathbf{v}_i^{\rightarrow}$ and $\mathbf{v}_i^{\leftarrow}$ is not equivalent to a formal reversal of the intracellular reaction direction in the biochemical network! Therefore, $\mathbf{v}^{\rightarrow}$, $\mathbf{v}^{\leftarrow}$ must always be kept strictly non-negative in computations.

Linear Constraints on Net Fluxes

Eq. (15) is a linear equation with respect to $\mathbf{x}$ that can be solved for $\mathbf{x}$, when all fluxes are known [cf. Eq. (22)]. To this end all available information on the metabolite fluxes must be supplied. This is done by formulating all assumptions made about these fluxes as linear constraints for $\mathbf{v}^{\text{net}}$ and $\mathbf{v}^{\text{xch}[0,1]}$. The arising set of constraints can be most conveniently expressed by using matrix notation, which has also been the key concept for metabolite flux balancing (van Heijden et al., 1994a). We start with the assumptions about net fluxes, which are formulated as:

$$\mathbf{N}^{\text{net}} \cdot \mathbf{v}^{\text{net}} = \mathbf{n}^{\text{net}} \quad (16)$$

with the *net flux constraint matrix* $\mathbf{N}^{\text{net}}$ and some given *constraint value vector* $\mathbf{n}^{\text{net}}$. Eq. (16) enables the following types of constraints to be expressed:

1. The stoichiometric equations for each intracellular metabolite pool are always automatically included in the net flux constraints, which is justified by assumption **(A2)** on metabolic stationarity. This means that the familiar stoichiometric matrix is a submatrix of $\mathbf{N}^{net}$ by default.
2. Energy balances for ATP, NADH, or NADPH can be expressed by constraint equations (van Heijden et al., 1994a) and even noninteger yield coefficients can be included in this way (Vallino and Stephanopoulos, 1993).
3. For the purpose of simulation studies a net flux $\mathbf{v}_i^{net}$ may be fixed at a given value n_i^{net}; that is, $\mathbf{v}_i^{net} = n_i^{net}$.

In the example, the stoichiometric equations are readily obtained from Eqs. (2) and can be interpreted as net flux balances for B and C:

$$\begin{aligned} \mathsf{B}: \quad & v_1^{net} = v_2^{net} + v_3^{net} \\ \mathsf{C}: \quad & v_2^{net} + v_3^{net} = v_4^{net} \end{aligned}$$

Additionally, $v_1^{net} = 1$ was fixed in the example study so that we arrive at the net flux constraint matrix and vector given by:

$$\mathbf{N}^{net} = \begin{pmatrix} 1 & -1 & -1 & . \\ . & 1 & 1 & -1 \\ 1 & . & . & . \end{pmatrix} \quad \text{and} \quad \mathbf{n}^{net} = \begin{pmatrix} . \\ . \\ 1 \end{pmatrix}$$

Linear Constraints on Exchange Fluxes

Similarly, linear constraints for exchange fluxes can be generally formulated as:

$$\mathbf{N}^{xch[0,1]} \cdot \mathbf{v}^{xch[0,1]} = \mathbf{n}^{xch[0,1]} \tag{17}$$

with a given *exchange flux constraint matrix*, $\mathbf{N}^{xch[0,1]}$, and an *exchange flux constraint value vector*, $\mathbf{n}^{xch[0,1]}$. Some commonly encountered assumptions are:

1. Unidirectionality of the ith reaction step; that is, $\mathbf{v}_i^{xch[0,1]} = 0$.
2. Rapid equilibrium of the ith reaction step, i.e., $\mathbf{v}_i^{xch[0,1]} = 1$.
3. Fixing of an exchange flux, i.e., $\mathbf{v}_i^{xch[0,1]} = n_i^{xch[0,1]}$ for some constant $n_i^{xch[0,1]}$.
4. Equality of exchange fluxes, i.e., $\mathbf{v}_i^{xch[0,1]} = \mathbf{v}_j^{xch[0,1]}$.

In the example, V_1, V_2, and V_4 were assumed to be unidirectional;

$$\mathbf{N}^{xch[0,1]} = \begin{pmatrix} 1 & . & . & . \\ . & . & 1 & . \\ . & . & . & 1 \end{pmatrix} \quad \text{and} \quad \mathbf{n}^{xch[0,1]} = \begin{pmatrix} . \\ . \\ . \end{pmatrix}$$

Free Fluxes

The linear constraint relations (16) and (17) will usually still not be sufficient for a complete determination of $\mathbf{v}^{net}$ and $\mathbf{v}^{xch[0,1]}$. To fix the remaining linear degrees of freedom some net and exchange fluxes must be identified that enable the constraint equations to be solved when values are supplied for them. These fluxes will henceforth be called the *free fluxes*. They are defined by an arbitrarily given set of additional constraints:

$$\mathbf{N}^{free} \cdot \begin{pmatrix} \mathbf{v}^{net} \\ \mathbf{v}^{xch[0,1]} \end{pmatrix} = \mathbf{n}^{free} \tag{18}$$

where $\mathbf{N}^{free}$ is composed from row unit vectors expressing which fluxes have been chosen. The free flux values, $\mathbf{n}^{free}$, may then be varied within simulation runs or for flux determination from measurements.

In the example, v_2^{net} and $v_2^{xch[0,1]}$ were chosen as free fluxes, i.e., we have:

$$\mathbf{N}^{free} = \left(\begin{array}{cccc|cccc} . & 1 & . & . & . & . & . & . \\ . & . & . & . & . & 1 & . & . \end{array}\right), \mathbf{n}^{free} = \begin{pmatrix} c_2^{net} \\ c_2^{xch[0,1]} \end{pmatrix}$$

Linking Eqs. (16), (17), and (18), we arrive at the combined linear constraint equation:

$$\mathbf{N} \cdot \begin{pmatrix} \mathbf{v}^{net} \\ \mathbf{v}^{xch[0,1]} \end{pmatrix} = \mathbf{n} \quad \text{with} \quad \mathbf{N} = \begin{pmatrix} \mathbf{N}^{net} & \mathbf{0} \\ \mathbf{0} & \mathbf{N}^{xch[0,1]} \\ & \mathbf{N}^{free} \end{pmatrix} \quad \text{and} \quad \mathbf{n} = \begin{pmatrix} \mathbf{n}^{net} \\ \mathbf{n}^{xch[0,1]} \\ \mathbf{n}^{free} \end{pmatrix} \tag{19}$$

If the free fluxes are chosen correctly these equations will uniquely determine all fluxes $\mathbf{v}^{net}$ and $\mathbf{v}^{xch[0,1]}$. To avoid pathological situations like insufficient, inconsistent, or redundant constraints, it is required that $\mathbf{N}$ is square and invertible. This is automatically checked within our software and can always be removed by changing the model formulation (cf. Chatterjee and Hadi, 1988; van Heijden et al., 1994a, 1994b; Vallino, 1991; Wiechert, 1996a). The reader may verify that, in the example, $\mathbf{N}$ (that is explicitly given in part II (Wiechert et al., 1996)) fulfills these conditions.

Linear Inequality Constraints

To exclude physiologically meaningless system states, like negative carbon fluxes, a set of inequality constraints is finally imposed on the system flux state. Again, some obligatory assumptions are always made; while others are optional:

1. Exchange fluxes are always restricted by $\mathbf{0} \leq \mathbf{v}^{xch[0,1]} \leq \mathbf{1}$.
2. The direction of a reaction step can be prescribed by requiring $\mathbf{v}_i^{net} > 0$ or $\mathbf{v}_i^{net} < 0$. For extracellular fluxes, the first assumption is obligatory.

3. The possible range for net fluxes should be restricted to prevent a numerical parameter fitting algorithm from searching in physiologically meaningless regions of the parameter space (see also Wiechert et al., 1997); i.e., $\mathbf{v}_i^{\text{net}} \le \overline{u}_i^{\text{net}}$ for some upper bound $\overline{u}_i^{\text{net}}$.
4. Similarly, exchange fluxes can be bounded to exclude the rapid equilibrium situation: $\mathbf{v}_i^{\text{xch}} \le \overline{u}_i^{\text{xch}}$.
5. In certain pathological situations, the network structure can become disconnected when fluxes vanish (Anderson, 1983). In the example this happens only in the trivial case $v_1^{\text{net}} = 0$. In this situation the carbon label balance equations [Eqs. (15)] have no unique solution, which can be prevented by assuming, e.g., $\mathbf{v}_i^{\text{net}} \ge \underline{u}_i^{\text{net}}$ for certain steps. See Anderson (1983) and Wiechert (1996a) for more details.

Because an inequality $a \le b$ can always be alternatively expressed as $-a \ge -b$ all constraints can be collected to a combined linear net flux inequality similar to Eq. (19):

$$\mathbf{U} \cdot \begin{pmatrix} \mathbf{v}^{\text{net}} \\ \mathbf{v}^{\text{xch}[0,1]} \end{pmatrix} \ge \mathbf{u} \tag{20}$$

In the example, we have:

$$\mathbf{U} = \left(\begin{array}{cccc|cccc} 1 & . & . & . & . & . & . & . \\ . & . & . & 1 & . & . & . & . \\ \hline . & . & . & . & 1 & . & . & . \\ . & . & . & . & -1 & . & . & . \\ . & . & . & . & . & 1 & . & . \\ . & . & . & . & . & -1 & . & . \\ . & . & . & . & . & . & 1 & . \\ . & . & . & . & . & . & -1 & . \\ . & . & . & . & . & . & . & 1 \\ . & . & . & . & . & . & . & -1 \end{array}\right) \quad \text{and}$$

$$\mathbf{u} = \begin{pmatrix} . \\ . \\ . \\ -1 \\ . \\ -1 \\ . \\ -1 \\ . \\ -1 \end{pmatrix}$$

A flux state ($\mathbf{v}^{\text{net}}$, $\mathbf{v}^{\text{xch}[0,1]}$), satisfying Eq. (20), is called *feasible*. Numerical methods for the computation of feasible solutions of linear inequalities are described elsewhere (Schuster and Schuster, 1993; Zoutendijk, 1991). However, if the imposed constraints are reasonable, feasible choices of $\mathbf{n}^{\text{free}}$ are usually intuitively clear. In the example, the feasible free fluxes are characterized by $v_2^{\text{net}} \le v_1^{\text{net}}$ [as obtained from Eq. (3)] and $0 \le v_2^{\text{xch}[0,1]} \le 1$ (by definition).

SOLVING THE MODEL EQUATIONS

Simulating a carbon labeling experiment means fixing the vector $\mathbf{n}^{\text{free}}$ of free fluxes at an arbitrarily given value and computing the natural flux state ($\mathbf{v}^{\rightarrow}$, $\mathbf{v}^{\leftarrow}$) and the label state $\mathbf{x}$ determined by this choice. To this end, the model equations have to be solved. Some numerical implementation details can be taken from Appendix B of Part II (Wiechert et al., 1996). The chosen simulation strategy consists of the following computation steps:

1. The inverse of the constraint matrix $\mathbf{N}$ is represented as:

$$\mathbf{N}^{-1} = (\mathbf{K}^{\text{net}} \quad \mathbf{K}^{\text{xch}[0,1]} \quad \mathbf{K}^{\text{free}})$$

where the submatrices have dim $\mathbf{n}^{\text{net}}$, dim $\mathbf{n}^{\text{xch}[0,1]}$, and dim $\mathbf{n}^{\text{free}}$ columns, respectively. Then, from Eq. (19):

$$\begin{aligned} &\begin{pmatrix} \mathbf{v}^{\text{net}} \\ \mathbf{v}^{\text{xch}[0,1]} \end{pmatrix} \\ &= \mathbf{N}^{-1} \begin{pmatrix} \mathbf{n}^{\text{net}} \\ \mathbf{n}^{\text{xch}[0,1]} \\ \mathbf{n}^{\text{free}} \end{pmatrix} \\ &= \mathbf{K}^{\text{free}} \cdot \mathbf{n}^{\text{free}} + \underbrace{\mathbf{K}^{\text{net}} \cdot \mathbf{n}^{\text{net}} + \mathbf{K}^{\text{xch}[0,1]} \cdot \mathbf{n}^{\text{xch}[0,1]}}_{\mathbf{k}^{\text{free}}} \\ &= \mathbf{K}^{\text{free}} \cdot \mathbf{n}^{\text{free}} + \qquad\qquad \mathbf{k}^{\text{free}} \\ &\overset{def}{=} \Psi(\mathbf{n}^{\text{free}}) \end{aligned} \tag{21}$$

Feasibility of the obtained solution is then checked with inequality (20) and infeasible choices of free flux values are rejected.
2. The application coordinates $\mathbf{v}^{\text{net}}$ and $\mathbf{v}^{\text{xch}}$ are computed by using the compactification $\mathbf{\Phi}_{\beta}^{[0,1]}$, and from this the natural flux state ($\mathbf{v}^{\rightarrow}$, $\mathbf{v}^{\leftarrow}$) is obtained by using the transformation $\mathbf{\Phi}$.
3. It can be generally shown that the system matrix $\sum_i \mathbf{v}_i^{\rightarrow} \cdot \mathbf{P}_i^{\rightarrow} + \sum_i \mathbf{v}_i^{\leftarrow} \cdot \mathbf{P}_i^{\leftarrow}$ in Eq. (15) is singular only when the carbon atom network becomes disconnected by virtue of vanishing fluxes (Anderson 1983). Because this situation should be excluded by inequality (20) it follows from the carbon flux balances (15):

$$\mathbf{x} = -\left(\sum_i \mathbf{v}_i^{\rightarrow} \cdot \mathbf{P}_i^{\rightarrow} + \sum_i \mathbf{v}_i^{\leftarrow} \cdot \mathbf{P}_i^{\leftarrow}\right)^{-1} \cdot \left(\sum_i \mathbf{v}_i^{\rightarrow} \cdot \mathbf{P}_i^{\text{inp}}\right) \cdot \mathbf{x}^{\text{inp}} \tag{22}$$

Thus the labeling state $\mathbf{x}$ is always a function of the natural flux state ($\mathbf{v}^{\rightarrow}$, $\mathbf{v}^{\leftarrow}$). This function is denoted by:

$$\Gamma: \begin{pmatrix} \mathbf{v}^{\rightarrow} \\ \mathbf{v}^{\leftarrow} \end{pmatrix} \rightarrow \mathbf{x} \tag{23}$$

Summarizing these steps a simulation run is essentially a sequence of the computational steps given by Eqs. (13), (14), (21), and (23):

$$\mathbf{n}^{\text{free}} \xrightarrow{\Psi} \begin{pmatrix} \mathbf{v}^{\text{net}} \\ \mathbf{v}^{\text{xch}[0,1]} \end{pmatrix} \xrightarrow{\Phi_{\beta}^{[0,1]}} \begin{pmatrix} \mathbf{v}^{\text{net}} \\ \mathbf{v}^{\text{xch}} \end{pmatrix} \xrightarrow{\Phi} \begin{pmatrix} \mathbf{v}^{\rightarrow} \\ \mathbf{v}^{\leftarrow} \end{pmatrix} \xrightarrow{\Gamma} \mathbf{x} \tag{24}$$

APPLICATION TO A REALISTIC METABOLIC NETWORK

The Cyclic Pentose Phosphate Pathway

The application of the previously introduced modeling and simulation strategy will now be illustrated by an example network of realistic complexity. This is the cyclic pentose phosphate pathway as encountered in xylose metabolizing microorganisms. Examples are the yeast *Pichia stipitis* (Ligthelm et al., 1988) and recently available mutants of *Zymomonas mobilis* (Zhang et al., 1995). These organisms are currently under investigation so that the following simulation studies are relevant for our NMR measurements that will be published in the future.

Figure 4a presents the underlying metabolic network and the involved reaction steps of substrate uptake, Upt, glycolysis, Gly_1–Gly_3, and pentose phosphate pathway, PPP_1–PPP_4. The corresponding carbon atom transitions are given in the Appendix. In the cyclic pathway the glycolytic step Gly_1 is reversed. The cycle is then closed via the PPP_1 step.

Because the pentose-phosphate isomerase and epimerase generally have a high activity (Wood, 1985) the pentose-phosphate pools (i.e., ribose-5-phosphate, ribulose-5-phosphate, and xylulose-5-phosphate) are lumped to a pool P5P. The substrate uptake step Upt, the efflux Gly_3 (leading to ethanol via pyruvate), and the steps PPP_1 and Gly_2 (each splitting a molecule into two parts) are assumed to be unidirectional for thermodynamic reasons. All other steps are considered bidirectional.

In practice, the precursor effluxes for biomass formation can all be directly determined from growth rate and biomass composition (Vallino and Stephanopoulos, 1993). However in the case of glycolysis and pentose phosphate pathway they usually make up only approximately 5% of the substrate uptake (Marx et al., 1996). It has been verified with simulation studies (not shown here) that their influence on the respective labels is very small. For this reason they were left out of the following considerations for simplicity.

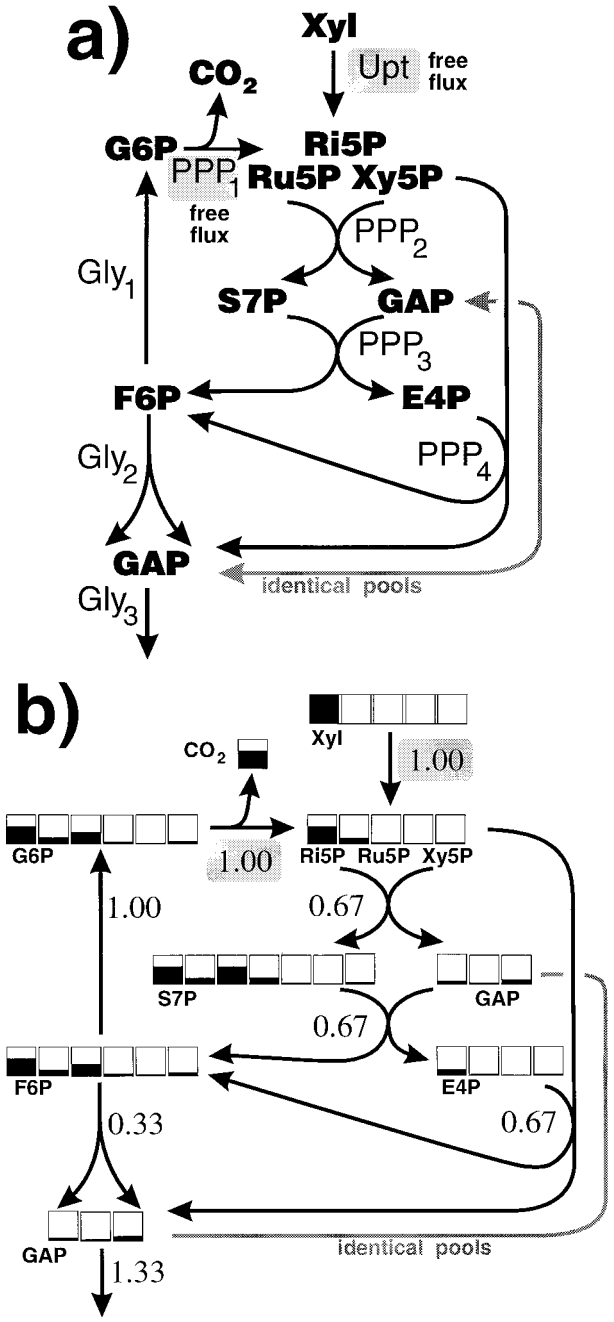

Figure 4. (a) Biochemical network of the cyclic pentose phosphate pathway as found in a mutant of *Zymomonas mobilis*. Notice that the GAP pool has been included twice. (b) Results of a simulation run with free fluxes, $upt^{\text{net}} = 1.0$ and $ppp_1^{\text{net}} = 1.0$, and all steps assumed to be unidirectional. Empty boxes represent positive carbon isotope enrichments below 3%.

The input metabolite, xylose, is supposed to be labeled at the first carbon atom position. It should be noticed that the label fractions, gap_2 and gap_3, can be easily measured in practice from the ethanol labeling, whereas any further labeling information must be gathered from cell components.

Balance Equations and Assumptions

For formulating the model equations a set of free fluxes must be chosen. The six stoichiometric balances for the eight unknown net fluxes leave two degrees of freedom for net fluxes that can be represented by the substrate uptake upt^{net} and the cycle flux ppp_1^{net} (the corresponding calculations are left out for shortness).

As is clear from Eq. (22), the system's labeling state is always left unchanged when all fluxes are multiplied by a constant. Thus, it is sufficient to scale all fluxes by setting $upt^{net} = 1$. Consequently, the transformation constant for $\mathbf{\Phi}_\beta^{[0,1]}$ is set as $\beta = 1$. Moreover, the directionality assumptions made above are given by:

$$upt^{xch[0,1]} = 0, ppp_1^{xch[0,1]} = 0, gly_2^{xch[0,1]} = 0, gly_3^{xch[0,1]} = 0$$

This finally leaves the free fluxes $ppp_1^{net}, ppp_2^{xch[0,1]}, ppp_3^{xch[0,1]}, ppp_4^{xch[0,1]}, gly_1^{xch[0,1]}$ for variation.

The most important inequality constraint (apart from the trivial relations ppp_1^{net}, $upt^{net} \geq 0$, and $0 \leq \mathbf{v}_i^{xch[0,1]} \leq 1$) is given by:

$$ppp_1^{net} \leq 2 \cdot upt^{net} = 2 \qquad (25)$$

It can be derived from the stoichiometric balances by using $gly_2^{net} \geq 0$. To this end, one observes that gly_2^{net} changes its sign if $ppp_1^{net} = 2 \cdot upt^{net}$. Finally, the substrate is labeled at the first carbon atom:

$$\mathbf{x}^{inp} = (1, 0, 0, 0, 0)^T$$

First Simulation Results

The simulation study starts with the special case of unidirectional fluxes as frequently assumed in the literature (Portais et al., 1993; Sharfstein et al., 1994; Zupke and Stephanopoulos, 1995) and an intermediate value for ppp_1^{net} [cf. Eq. (25)]:

$$ppp_2^{xch[0,1]} = ppp_3^{xch[0,1]} = ppp_4^{xch[0,1]} = gly_1^{xch[0,1]} = 0, \quad ppp_1^{net} = 1 \qquad (26)$$

Applying the solution strategy of Eq. (24) leads to the fluxes and labeling enrichments shown in Figure 4b. The first result is that all intracellular pools become labeled even with no reversible step being present.

This simulation run is now taken as the starting point for further variation studies in the investigation of the free flux influence on the system's state. From now on we concentrate on the flux information that can be obtained from gap_2, gap_3 (which can be easily measured), and $e4p_1$. All other pools led to less significant results and are not shown here for shortness. In practice, the carbon enrichment in E4P can be obtained from its successor phenylalanine isolated from cell protein. Moreover, it should be mentioned that the CO_2 production in the oxidative pentose phosphate pathway is not necessarily measurable because CO_2 is involved in many other reaction steps outside the considered section of the central metabolism.

As a first variation it is now investigated whether the cycle flux ppp_1^{net} can be determined from the given labeling data at least in the situation where all fluxes are still unidirectional. Figure 5a shows what happens when ppp_1^{net} is varied in the feasible range [0, 2]. As can be seen, gap_1, gap_3, and $e4p_1$ monotonously depend on

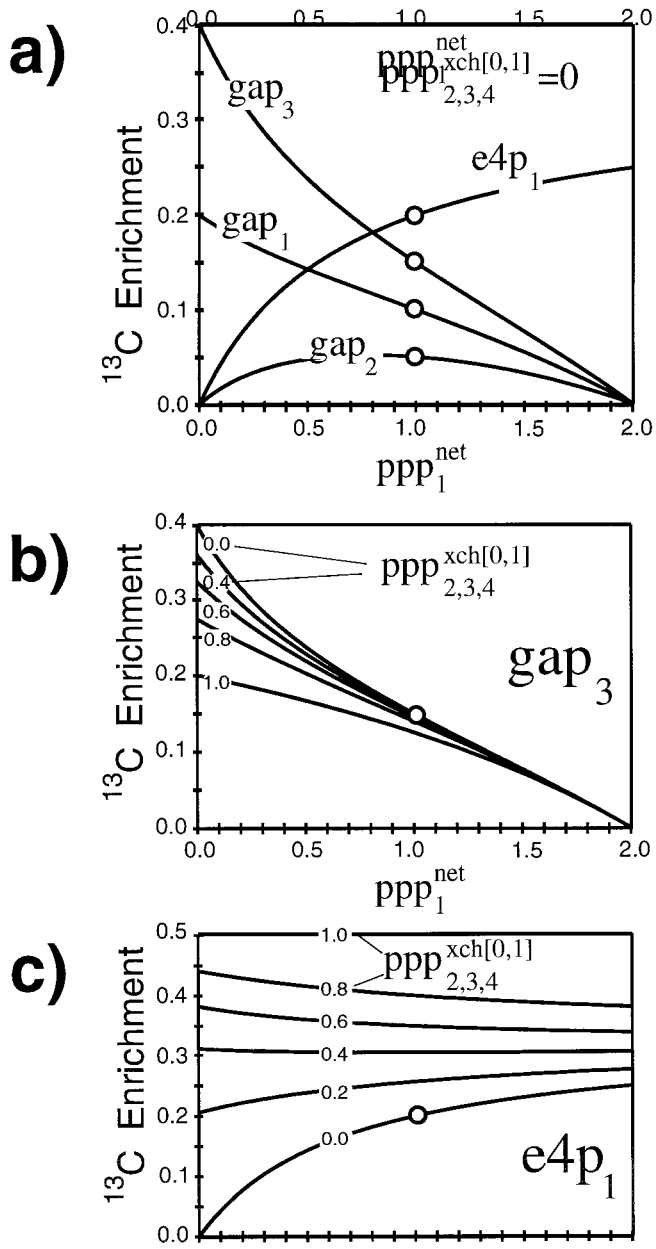

Figure 5. Results of parameter variation studies with $upt^{net} = 1.0$, $ppp_2^{xch} = ppp_2^{xch} = ppp_4^{xch} = ppp_{2,3,4}^{xch}$, and all other fluxes assumed to be unidirectional. (a) Fractional labeling gap_1, gap_2, gap_3, $e4p_1$ as a function of ppp_1^{net} for $ppp_{2,3,4}^{xch} = 0.0$. (b) gap_3. (c) $e4p_1$ as a function of ppp_1^{net} and $ppp_{2,3,4}^{xch}$. The labeling situation of Figure 4b is marked in each plot.

ppp_1^{net} in contrast to gap_2. Consequently, ppp_1^{net} can be uniquely determined from a measurement of gap_3 or $e4p_1$, but not from gap_2.

Another important property of the carbon label enrichment that can be concluded from Figure 5a is that, in case of the assumed Eqs. (26):

$$2 \cdot gap_1 = gap_2 + gap_3 \tag{27}$$

holds for any value of ppp_1^{net}. This means that gap_1 cannot help to identify further fluxes when gap_2 and gap_3 are already available. However, the additional measurement may help to improve the statistical quality of the determined fluxes, which is discussed in Part II (Wiechert et al., 1997) in more depth. General algorithms for computing such algebraic redundancy relations are discussed elsewhere (Wiechert, 1995, 1996b; Wiechert and de Graaf, 1996).

The Influence of Exchange Fluxes

Another variation study revealed that $gly_1^{xch[0,1]}$ has no influence on the system's labeling state at all. Indeed, from the metabolite flux balance $gly_1^{\leftarrow} + ppp_1^{\rightarrow} = gly_1^{\rightarrow}$ and the carbon labeling balance equations it follows for all $i = 1, \ldots, 6$:

$$\begin{aligned} gly_1^{\rightarrow} \cdot f6p_i &= (gly_1^{\leftarrow} + ppp_1^{\rightarrow}) \cdot g6p_i \\ &= gly_1^{\rightarrow} \cdot g6p_i \Rightarrow g6p_i = f6p_i \end{aligned}$$

This proves that the exchange flux $gly_1^{xch[0,1]}$ is not identifiable from labeling data and extracellular fluxes, and thus the Gly_1 step can be fixed to $gly_1^{xch[0,1]} = 0$ without affecting the results obtained below. A less trivial example of nonidentifiable fluxes in the anaplerotic pathway is presented in Wiechert (1996b); some principles of algebraic identifiability analysis for carbon labeling systems are given in Wiechert (1995).

To illustrate the influence of the remaining free fluxes with only 2 degrees of freedom, the pentose phosphate pathway exchange fluxes are now set at the same nonzero value denoted by $ppp_{2,3,4}^{xch[0,1]}$:

$$ppp_2^{xch[0,1]} = ppp_3^{xch[0,1]} = ppp_4^{xch[0,1]} \stackrel{def}{=} ppp_{2,3,4}^{xch[0,1]}$$

Although this does not enable the full variety of exchange effects to be demonstrated it proved a very illustrative choice for understanding the system's properties. The full complexity will be treated numerically in Part II (Wiechert et al., 1997).

Figure 5b and c shows the results for the gap_3 and $e4p_1$ label fractions when the cycle flux ppp_1^{net} and the common exchange flux $ppp_{2,3,4}^{xch[0,1]}$ are both varied. Surprisingly, gap_3 remains a monotonously decreasing function of ppp_1^{net} for all exchange values, whereas the slope of $e4p_1$ changes its sign with increasing $ppp_{2,3,4}^{xch[0,1]}$. For cycle fluxes of approximately $ppp_1^{net} > 1$ the gap_3 label is rather insensitive with respect to the exchange fluxes. In this situation, ppp_1^{net} can still be accurately determined from gap_3. However, for small values of ppp_1^{net}, a single fractional labeling measurement is no more sufficient for its determination because exchange fluxes have a strong influence on the labeling state.

The superposed contour plot technique is used for investigating the potential of two simultaneously measured label fractions. As opposed to Figure 2, where the flux state contour lines in the labeling space were given, Figure 6 shows the labeling state contour lines in the flux space. This graphical representation is more suitable for investigating flux identifiability because the labeling state is always uniquely determined by the flux state according to Eq. (22), but not vice versa, as shown by Figure 5a.

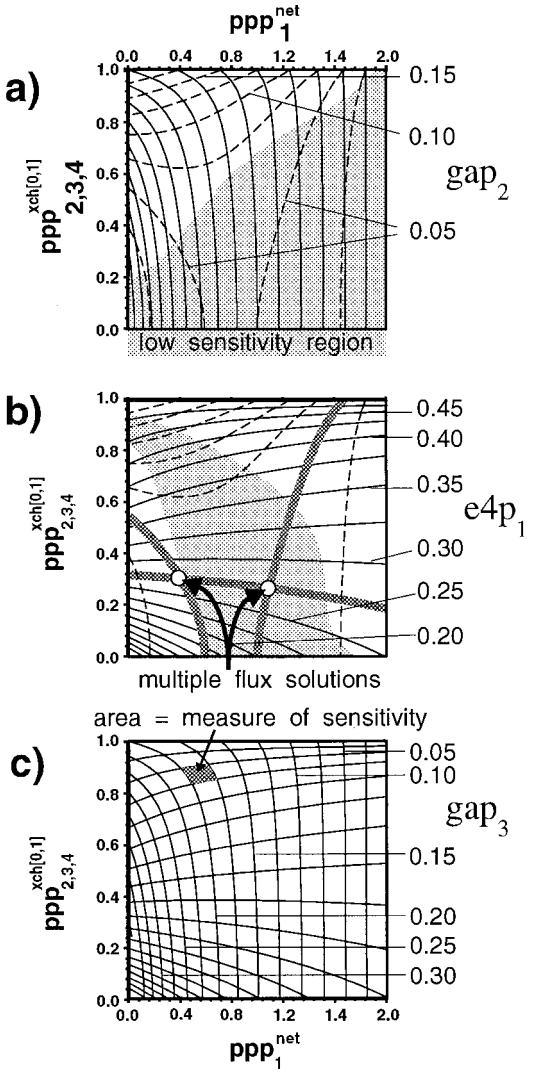

Figure 6. Superposition of contour plots for investigating identifiability and sensitivity of fluxes ppp_1^{net} and $ppp_{2,3,4}^{xch}$ with respect to measured fractional labels: (a) gap_2 contour lines (dashed and labeled) superposed with gap_3 contour lines [full with labeling as in (c)]; (b) gap_2 contour lines [dashed with labeling as in (a)] superposed with $e4p_1$ contour lines (full and labeled); (c) gap_3 contour lines (labeled) superposed with $e4p_1$ contour lines [with labeling as in (b)].

Figure 6a shows that the free fluxes given by ppp_1^{net} and $ppp_{2,3,4}^{xch[0,1]}$ are uniquely determined by gap_2 and gap_3. However, the sensitivity of the common exchange flux, $ppp_{2,3,4}^{xch[0,1]}$, with respect to measurement errors is, in general, so large that only the order of magnitude can be determined (low sensitivity regions are characterized by large cells in the contour grid). On the other hand, ppp_1^{net} is comparatively well determined in all situations.

Figure 6b shows that the combination of gap_2 and $e4p_1$ does not enable the free fluxes to be uniquely determined (cf. Zupke and Stephanopoulos, [1994] for a similar example). For certain label outcomes there are two possible solutions of the flux determination problem. On the other hand, in most uniquely determined cases, the sensitivity of the determined solution is considerably better than that in Figure 6a.

Figure 6c shows that measurements of gap_3 and $e4p_1$ are best suited to determine ppp_1^{net} and $ppp_{2,3,4}^{xch[0,1]}$. Obviously, the free fluxes are now always uniquely determined and have a good statistical quality as well. All other combinations of two labeling measurements in the system could not produce an equally adequate flux determination. An in-depth treatment of the statistical properties of flux estimates is given in Part II (Wiechert et al., 1997).

Some General Consequences

The most important consequence of this simulation study is that one has to be aware of bidirectional reaction steps that significantly influence the systems labeling state in realistic metabolic networks. In the example, the flux estimates obtained with unidirectionality assumptions from Figure 5a are strongly biased when significant exchange fluxes are present. This is expected to be extremely relevant for flux quantitation in the pentose phosphate pathway.

Concerning the general problem of flux determination from measured extracellular fluxes and fractional labels some principal nonlinear phenomena have been exemplified that must be expected for any realistic network:

1. For the determination of absolute flux values at least one net flux must be directly measured as follows from Eq. (22).
2. Clearly, the number of measurements to be made must at least equal the degrees of freedom in the simulation runs; that is, the number of free fluxes.
3. Even if this number is large enough there may be algebraic measurement redundancies like Eq. (27) reducing the amount of available information.
4. Even if such redundancies do not occur the fluxes may still not be uniquely identifiable (Fig. 6b).
5. Even when the data are sufficient for a unique flux determination this does not guarantee a good statistical quality because sensitivities may be very low (Fig. 6a).

Consequently, as much labeling data as possible should be gathered to obtain a unique flux estimate with good statistical quality (Fig. 6c).

CONCLUSIONS

We have shown that stationary metabolic carbon isotope labeling experiments offer a rich source of information, which enables intracellular fluxes in the central metabolism, together with exchange fluxes, to be determined. No assumptions about enzyme kinetics or energy balances are required although energy balancing can be also included in our formalism.

We have presented a general modeling framework for carbon labeling experiments that extends the familiar metabolite flux balancing technique and is capable of expressing all assumptions on carbon labeling systems that can be found in the literature. Our simulation studies have proven that labeling systems expose strong nonlinearities, and for this reason pose many problems that are not known from metabolite flux balancing. In particular, the incorporation of bidirectional reaction steps leads to severe computational problems that could be solved by a suitable compactification transformation. Moreover, for practical applications, multiple flux solutions based on given measurements and state-dependent sensitivities have to be expected.

We successfully solved the problems of automatic equation synthesis, numerically stable state computation, and simulation of carbon labeling experiments by supplying a flexible compiler tool for the automatic generation of all balance equations and assumed relations (cf. Appendix) accompanied by highly sophisticated numerical algorithms that are described in Appendix B of Part II (cf. Wiechert [1996b] for more details).

APPENDIX: FORMAL REPRESENTATION OF METABOLIC LABELING SYSTEMS

The main advantage of the general structural representation of carbon labeling systems presented in this study is the opportunity for automatic generation of all required structures from a formal textual input. Thus, parametric and structural variation studies can be performed rapidly and all assumptions made in the modeling process can be documented precisely. In this Appendix, some details of the formal language established for simulating labeling systems are given. This language is processed by a specialized compiler program that produces all required vectors and matrices from a textual input. More information on the programs can be obtained from the authors.

Reaction Equations and Carbon Atom Transitions

All reactions in the metabolic pathways of interest are given in familiar biochemical sum notation. As an exam-

ple, the transaldolase reaction from the pentose phosphate pathway is written as (cf. Zupke and Stephanopoulos, 1994):

$$PPP_3\text{: GAP} + \text{S7P} \rightarrow \text{E4P} + \text{F6P}$$

The corresponding forward and backward fluxes are then automatically incorporated into the system model by the compiler program. A positive net flux means that the reaction takes place in the direction indicated by the arrow. Further directionality assumptions can be formulated as in the ''Expressing Constraints'' section.

Tracing carbon atoms through a metabolic network additionally requires knowing their fate within each chemical reaction step. To this end, the corresponding atom transitions have to be supplied. For example, the transaldolase step is expressed completely as:

$$\begin{aligned} PPP_3\text{: GAP} + \text{S7P} &\rightarrow \text{E4P} + \text{F6P} \\ \#ABC + \#abcdefg &\rightarrow \#defg + \#abcABC \end{aligned}$$

This means that the first carbon atom of GAP (denoted here by A) becomes the fourth carbon atom of F6P and so on. The characters in the second line can be freely chosen, but must clearly be distinct for each metabolite participating in the reaction. Both integer and noninteger stoichiometric coefficients can be incorporated into the equations as, for example, in an ATP production step:

$$\text{ATPProd: } 2.1\ \text{NADH} + \text{ADP} \rightarrow 2.1\ \text{NAD} + \text{ATP}$$

Clearly, this only makes sense when no corresponding carbon atoms have to be traced through the network.

Formal Expression of Special Metabolic Situations

Certain constructs found in the literature can now be expressed within the formal language as follows:

- Carbon atom transitions for bimolecular reactions of type:

  $$PPP_2\text{: } 2\ \text{P5P} \rightarrow \text{S7P} + \text{GAP}$$

  (P5P denoting the lumped pentose phosphate pool) can be expressed by doubling P5P while using different carbon atom symbols (cf. Zupke and Stephanopoulos, 1994):

  $$\begin{aligned} PPP_2\text{: P5P} + \text{P5P} &\rightarrow \text{S7P} + \text{GAP} \\ \#ABCDE + \#abcde &\rightarrow \#ABabcde + \#CDE \end{aligned}$$

- The stoichiometry of biomass production is frequently expressed by noninteger coefficients (see, e.g., Vallino and Stephanopoulos, 1993). This should be alternatively expressed by introducing a separate efflux into the biomass for each cell component, thus enabling the tracing of carbon atoms as follows:

  $$\begin{aligned} \text{G6PEffl: G6P} &\rightarrow \text{G6PBiomass} \\ \#ABCDEF &\rightarrow \#ABCDEF \end{aligned}$$

  The ''stoichiometric coefficient'' obtained from the biomass production rate and cell composition data is then supplied as a measured value for G6PEffl.
- Reactions with symmetric metabolites have drawn much attention in the modeling of isotope labeling experiments (Sumegi et al., 1993). A well-known example is the fumarase step in the citric acid cycle. Because fumarate is completely symmetric we must consider two ''label scrambling'' reactions:

  $$\begin{aligned} \text{ScrA: FUM} &\rightarrow \text{MAL} \qquad \text{ScrB: FUM} \rightarrow \text{MAL} \\ \#ABCD &\rightarrow \#ABCD \qquad\quad \#ABCD \rightarrow \#DCBA \end{aligned}$$

  However, both reactions take place at the same rate, which can easily be expressed by an additional equality constraint later on.

Expressing Constraints

Several equality and inequality flux constraint equations are automatically generated by the compiler program and thus need not be explicitly supplied:

1. The metabolite flux balances.
2. The unidirectionality of an input or output flux with number i, i.e., $\mathbf{v}_i^{\text{xch}[0,1]} = 0$.
3. The direction for an extracellular flux, i.e., $\mathbf{v}_i^{\text{net}} \geq 0$.
4. The trivial inequalities $0 \leq \mathbf{v}_i^{\text{xch}} \leq 1$ for all exchange fluxes.

Arbitrary further constraints can be given. A complete example, including additional constraints, is given next.

Pentose Phosphate Pathway Example

As a completely documented example the cyclic pentose phosphate pathway from Figure 4 is formulated. A hierarchical input format enables all equations and assumptions to be given in a structured manner:

```
EQUATIONS
{
  Upt:   Glu                  → GP6
         #ABCDEF              → #ABCDEF                ;
  Gly1:  F6P                  → G6P
         #ABCDEF              → #ABCDEF                ;
  Gly2:  F6P                  → GAP      + GAP
         #ABCDEF              → #CBA     + #DEF        ;
  Gly3:  GAP                  → Pyr
         #ABC                 → #ABC                   ;
  PP1:   G6P                  → CO2      + P5P
         #ABCDEF              → #A       + #BCDEF      ;
  PP2:   P5P      + P5P       → S7P      + GAP
         #ABCDE   + #abcde    → #ABabcde + #CDE        ;
  PP3:   GAP      + S7P       → E4P      + F6P
         #ABC     + #abcdefg  → #defg     + #abcABC     ;
  PP4:   P5P      + E4P       → GAP      + F6P
         #ABCDE   + #abcd     → #CDE     + #ABabcd     ;
}
```

```
NET_FLUXES
{
    FREE
    {
        PPP1;
    }
    EQUALITIES
    {
        Upt=1;
    }
    INEQUALITIES
    {
        PPP2>=0;
        PPP3>=0;
        PPP4>=0;
    }
}
```

```
EXCHANGE_FLUXES
{
    FREE
    {
        PPP2;
    }
    EQUALITIES
    {
        PPP2=PPP3;
        PPP3=PPP4;
        Gly1=0;
        Gly2=0;
    }
    INEQUALITIES
    {
    }
}
```

References

Ahlfors, L. V. 1979. Complex analysis. 3rd edition. McGraw Hill, New York.

Anderson, D. H. 1983. Compartmental modelling and tracer kinetics, vol. 50. In: Lecture notes in biomathematics. Springer, New York.

Bailey, J. E. 1991. Towards a science of metabolic engineering. Science **252**: 1668–1674.

Blum, J. J., Stein, R. B. 1982. On the analysis of metabolic networks, pp. 99–124. In: R. F. Goldberger (eds.), Biological regulation and development, vol. 3A. Plenum, Press, New York.

Chatham, J. C., Forder, J. R., Glickson, J. D., Chance, E. M. 1995. Calculation of absolute metabolic fluxes and the elucidation of the pathways of glutamate labeling in perfused rat heart by ^{13}C NMR spectroscopy and nonlinear least squares analysis. J. Biol. Chem. **270**: 7999–8008.

Chatterjee, S., Hadi, A. S. 1988. Sensitivity analysis in linear regression. John Wiley & Sons, New York.

Crawford, J. M., Blum, J. J. 1983. Quantitative analysis of flux along the gluconeogenic, glycolytic and pentose phosphate pathways under reducing conditions in hepatocytes isolated from fed rats. Biochem. J. **212**: 595–598.

Eisenreich, W., Strauss, G., Werz, U., Fuchs, G., Bacher, A. 1993. Retrobiosynthetic analysis of carbon fixation in the phototrophic eubacterium *Chloroflexus aurantiacus.* Eur. J. Biochem. **215**: 619–632.

Ekiel, I., Smith, I. C. P., Sprott, G. D. 1983. Biosynthetic pathways in *Methanospirillum hungatei* as determined by ^{13}C nuclear magnetic resonance. J. Bacteriol. **156**: 316–326.

Goel, A., Ferrance, J., Jeong, J., Ataai, M. M. 1993. Analysis of metabolic fluxes in batch and continuous cultures of *Bacillus subtilis.* Biotechnol. Bioeng. **42**: 686–696.

van Heijden, R. T. J. M., Heijnen, J. J., Hellinga, C., Romein, B., Luyben, K. C. A. M. 1994a. Linear constraint relations in biochemical reaction systems: I. Classification of the calculability and the balanceability of conversion rates. Biotechnol. Bioeng. **43**: 3–10.

van Heijden, R. T. J. M., Romein, B., Heijnen, J. J., Hellinga, C., Luyben, K. C. A. M. 1994b. Linear constraint relations in biochemical reaction systems: II. Diagnosis and estimation of gross errors. Biotechnol. Bioeng. **43**: 11–20.

Hofmeyr, J. H. S. 1986. Steady-state modelling of metabolic pathways: a guide for the prospective simulator. Comp. Appl. Biosci. **2**: 5–11.

Holzhutter, H. G. 1985. Compartmental analysis: theoretical aspects and applications. Biomed. Biochim. Acta **44**: 863–873.

Jorgensen, H. 1995. Metabolic flux distributions in *Penicillium chrysogenum* during fed-batch cultivations. Biotechnol. Bioeng. **46**: 117–131.

Lambrecht, R. M., Rescigno, A. (eds.) 1983. Tracer kinetics and physiological modelling. In: Lecture notes in biomathematics (no. 48). Springer, New York.

O'Leary, M. H. 1982. Heavy-atom isotope effects on enzyme-catalyzed reactions, pp. 67–75. In: H. L. Schmidt, H. Forstel, and K. Heinzinger (eds.), Analytical chemistry symposia series, vol. 11. Elsevier, Amsterdam.

Ligthelm, M. E., Prior, B. A., du Preez, J. C., Brandt, V. 1988. An investigation of D-[1-^{13}C] xylose metabolism in *Pichia stipitis* under aerobic and anaerobic conditions. Appl. Microbiol. Biotechnol. **28**: 293–296.

Marx, A., de Graaf, A. A., Wiechert, W., Eggeling, L., Sahm, H. 1996. Determination of the fluxes in central metabolism of *Corynebacterium glutamicum* by NMR spectroscopy combined with metabolite balancing. Biotechnol. Bioeng. **49**: 111–129.

Mavrovouniotis, M. L. 1991. Estimation of standard Gibbs energy changes of biotransformations. J. Biol. Chem. **266**: 14440–14445.

Portais, J.-C., Schuster, R., Merle, M., Canioni, P. 1993. Metabolic flux determination in C6 glioma cells using carbon-13 distribution upon [1-^{13}C] glucose incubation. Eur. J. Biochem. **217**: 457–468.

Rabkin, M., Blum, J. J. 1985. Quantitative analysis of intermediary metabolism in hepatocytes incubated in the presence and absence of glucagon with a substrate mixture containing glucose, ribose, fructose, alanine and acetate. Biochem. J. **225**: 761–786.

Reder, C. 1988. Metabolic control theory: a structural approach. J. Theor. Biol. **135**: 175–201.

Rizzi, M., Theobald, U., Querfurth, E., Rohrhirsch, T., Baltes, M., Reuss, M. 1996. In vivo investigations of glucose transport in *Saccharomyces cerevisiae.* Biotechnol. Bioeng. **49**: 316–327.

Roels, J. A. 1983. Energetics and kinetics in biotechnology. Elsevier, Amsterdam.

Schmidt, H.-L., Forstel, H., Heinzinger, K. (eds.) 1982. Stable isotopes. Analytical chemistry symposia series, vol. 11. Elsevier, Amsterdam.

Schugerl, K. (ed.) 1991. Biotechnology. Measuring, modelling and control, vol. 4. 2nd edition. Verlag Chemie, Weinheim.

Schuster, R., Schuster, S., Holzhutter, H.-G. 1992. Simplification of complex kinetic models used for the quantitative analysis of nuclear magnetic resonance or radioactive tracer studies. J. Chem. Soc. Faraday Trans. **88**: 2837–2844.

Schuster, R., Schuster, S. 1993. Refined algorithm and computer program for calculating all non-negative fluxes admissible in steady state of biochemical reaction systems with or without some flux rates fixed. Comp. Appl. Biosci. **9**: 79–85.

Sharfstein, S. T., Tucker, S. N., Mancuso, A., Blanch, H. W., Clark, D. S. 1994. Quantitative in vivo nuclear magnetic resonance studies of hybridoma metabolism. Biotechnol. Bioeng. **43**: 1059–1074.

Stein, R. B., Blum, J. J. 1979. Quantitative analysis of intermediary metabolism in *Tetrahymena*—cells grown in proteose–peptone and resuspended in a defined nutrient-rich medium. J. Biol. Chem. **254**: 10385–10395.

Stephanopoulos, G., Vallino, J. J. 1991. Network rigidity and metabolic engineering in metabolite overproduction. Science **252**: 1675–1681.

Stephanopoulos, G., Sinskey, A. J. 1993. Metabolic engineering—methodologies and future prospects. Tib Tech **11**: 392–396.

Stryer, L. 1988. Biochemistry. 3rd edition. W. H. Freeman Co., New York.

Sumegi, B., Sherry, A. D., Malloy, C. R., Srere, P. A. 1993. Evidence for orientation-conserved transfer in the TCA cycle in *Saccharomyces cerevisiae:* ^{13}C NMR studies. Biochemistry **32**: 12725–12729.

Szyperski, T. 1995. Biosynthetically directed fractional ^{13}C-labeling of proteinogenic amino acids—an efficient analytical tool to investigate intermediary metabolism. Eur. J. Biochem. **232**: 433–448.

Vallino, J. J. 1991. Identification of branch-point restrictions in microbial metabolism through metabolic flux analysis and local network perturbations, Ph.D. thesis, Massachusetts Institute of Technology, Cambridge, MA, USA.

Vallino, J. J., Stephanopoulos, G. 1993. Metabolic flux distribution in *Corynebacterium glutamicum* durng growth and lysine overproduction. Biotechnol. Bioeng. **41**: 633–646.

Varma, A., Palsson, B. O. 1994. Metabolic flux balancing: basic concepts, scientific and practical use. Bio/Technol. **12**: 994–998.

Westerhoff, H. V., van Dam, K. 1987. Mosaic nonequilibrium thermodynamics and control of biological free-energy transduction. Elsevier, Amsterdam.

Weuster-Botz, D., de Graaf, A. A. 1996. Reaction engineering methods to study intracellular metabolite concentrations. Adv. Biochem. Eng. Biotechnol. **54**: 76–108.

Wiechert, W. 1994. Design of a software framework for flux determination by ^{13}C NMR isotope labelling experiments, pp. 305–310. In: E. Gnaiger, F. N. Gellerich, and M. Wyss (eds.), What is controlling life? Modern trends in biothermokinetics, vol. 3. Innsbruck University Press, Innsbruck, Austria.

Wiechert, W. 1995. Algebraic methods for the analysis of redundancy and identifiability in metabolic ^{13}C labelling systems, pp. 169–184. In: D. Schomburg and U. Lessel (eds.), Bioinformatics; from nucleic acids and proteins to cell metabolism. Verlag Chemie, Weinheim.

Wiechert, W. 1996a. Metabolische Kohlenstoff-Markierungssysteme—Modellierung, Simulation, Analyse, Datenauswertung. Habilitationsschrift, University of Bonn, Bonn, Germany.

Wiechert, W. 1996b. Metabolic flux determination by stationary ^{13}C tracer experiments: analysis of sensitivity, identifiability and redundancy, pp. 128–135. In: J. Dolezal and J. Fidler (eds.), System modelling and optimization. Chapman & Hall, London.

Wiechert, W., de Graaf, A. A. 1993. Modelling of ^{13}C labelling in metabolic pathways for in vivo flux analysis using NMR, pp. 19–24. In: V. Bales (ed.), Modelling for improved bioreactor performance. Male Centrum, Bratislava.

Wiechert, W., de Graaf, A. A., Marx, A. 1995. In vivo stationary flux determination using ^{13}C NMR isotope labelling experiments. In: A. Munack and K. Schugerl (eds.), Computer applications in biotechnology. Pergamon Press, New York.

Wiechert, W., de Graaf, A. A. 1996. In vivo stationary flux analysis by ^{13}C labelling experiments. Adv. Biochem. Eng. Biotechnol. **54**: 109–154.

Wiechert, W., Siefke, C., de Graaf, A. A., Marx, A. 1997. Bidirectional reaction steps in metabolic networks: II. Flux estimation and statistical analysis. Biotechnol. Bioeng. **55**: 118–135.

Winkler, F. J., Kexel, H., Kranz, C., Schmidt, H.-L. 1982. Parameters affecting the $^{13}CO_2/^{12}CO_2$ discrimination of the ribulose-1,5-bisphosphate carboxylase reaction, pp. 83–89. In: H.-L. Schmidt, H. Forstel, and K. Heinzinger (eds.), Analytical chemistry symposia series, vol. 11. Elsevier, Amsterdam.

Wood, T. 1985. The pentose phosphate pathway. Academic Press, New York.

Zhang, M., Eddy, C., Deanda, K., Finkelstein, M., Picataggio, S. 1995. Metabolic engineering of a pentose metabolism pathway in ethanologenic *Zymomonas mobilis*. Science **267**: 240–243.

Zoutendijk, G. 1991. Mathematical programming methods. North Holland, Amsterdam.

Zupke, C., Stephanopoulos, G. 1994. Modeling of isotope distributions and intracellular fluxes in metabolic networks using atom mapping matrices. Biotechnol. Prog. **10**: 489–498.

Zupke, C., Stephanopoulos, G. 1995. Intracellular flux analysis in hybridomas using mass balances and in vitro ^{13}C NMR. Biotechnol. Bioeng. **45**: 292–303.